NOTES AND CORRESPONDENCE

Analysis of the Arctic Oscillation Simulated by AGCM

By Koji Yamazaki[1] and Yasuhiro Shinya[2]

Graduate School of Environmental Earth Science, Hokkaido University, Sapporo, 060-0810 Japan

(Manuscript received 5 April 1999, in revised form 9 August 1999)

Abstract

The annular mode in the Northern Hemisphere (NH) extratropical circulation, which has an equivalent barotoropic structure from the surface to the lower stratosphere, is called the Arctic Oscillation (AO), by Thompson and Wallace (1998). The AO is the leading empirical orthogonal function (EOF) mode of the sea level pressure field, and it can be seen throughout the year. It is more dominant in winter. It is characterized as a seesaw pattern of mass, between the Arctic region and the midlatitude belt. It is also a seesaw of the mean zonal wind, between the region poleward of 40°N and that equatorward of it.

In this study, an analysis of the simulated AO is made, to confirm that the AO is an atmospheric internal mode, and for studying the transition mechanism to the high/low polarity of the AO. The seasonal and perpetual February runs were made by using the Center for Climate System Research/National Institute for Environmental Studies (CCSR/NIES) atmospheric general circulation model (AGCM). In both runs, the AO signature is dominant. Its magnitude is similar to the observed one. Thus, it is confirmed that the AO is an internal mode of the atmosphere. Using data from a perpetual February integration, a composite analysis of the transition to the high/low polarity of the AO is made.

Based upon the transformed Eulerian mean equation for the mean zonal wind, it is investigated which term is responsible for the transition. The results indicate that the wave forcing term contributes to the transition and the term of the residual meridional circulation acts to restore the transition. A decomposition of the wave forcing to zonal wave component indicates that planetary-scale wavenumbers 2 and 3 contribute most to the transition. The synoptic-scale waves contribute partly to the low-latitude wind change.

In the perpetual February run, a slowly propagating AO-related stratosphere-troposphere coupled mode, is detected. Its oscillation period is 4–6 months. The anomaly of the zonal-mean, zonal wind first appears in the subtropical stratosphere and propagates poleward. Once the anomaly reaches high latitude, it becomes large and propagates into the troposphere.

1. Introduction

Recent studies have shown that there exist several modes of climate variability in timescales from intraseasonal to interdecadal. There are at least two types of fundamentally different modes of climate variability internal to the atmosphere: wavelike teleconnection patterns, and annular modes, both of which owe their existence to different dynamical processes. For example, the Pacific/North American (PNA) pattern is classified as the former type. The Arctic Oscillation (AO) is a climate mode of the latter type.

Thompson and Wallace (1998, 1999a, hereafter refered as TW98 and TW99a), applied an empirical orthogonal function (EOF) analysis to the wintertime monthly-mean sea level pressure (SLP) field in the NH, and obtained an annular mode as the first EOF. By applying a regression technique to other levels and other variables, they studied the vertical structure of this mode. They found that it has an equivalent barotropic structure, from the surface to the lower stratosphere. They named this mode the Arctic Oscillation. The AO is a north-south seesaw of the mass, between the Arctic region poleward of 60°N and the surrounding zonal ring. The AO is also a north-south seesaw of zonal-mean, zonal wind, between around 35°N and 60°N. The AO is the variation in the strength of the polar vor-

Corresponding author: Koji Yamazaki, Graduate School of Environmental Earth Science, Hokkaido University, Sapporo, 060-0810 Japan. E-mail: yamazaki@ees.hokudai.ac.jp

1 Additional affiliation: IARC, Frontier Research System for Global Change

2 Present affiliation: Fujitsu Limited

tex. Before TW98, many studies were made on this pattern, mostly as a troposphere-stratosphere coupled mode (Baldwin *et al.*, 1994, Perlwitz and Graf, 1995, Kodera *et al.*, 1996, Kitoh *et al.*, 1996).

The spatial pattern of the AO at sea level pressure, is similar to the pattern associated with the North Atlantic Oscillation (NAO), but the AO pattern has a more zonally symmetric structure. The surface air temperatures over Eurasia, are closely related to the AO or NAO (Hurrel, 1995, Koide and Kodera, 1999). The AO is not closely related to sea surface temperatures (SSTs) in the tropics (Kodera *et al.*, 1996, Koide and Kodera, 1999), and it is simulated in atmospheric general circulation models (AGCMs) with climatological SSTs (Kodera *et al.*, 1996). These facts indicate that the AO is basically an internal mode in the atmosphere, and is caused without variations of boundary, and/or external forcings.

TW99a showed that the anomalous upward motion in the Arctic region, the equatorward motion in the high-latitude upper troposphere and the poleward motion in the high-latitude lower troposphere, are associated with the high polarity of the AO index, *i.e.*, the stronger polar vortex. The poleward motion in the lower troposphere, acts to increase the mean zonal flow through Coriolis force. It is preferable for maintaining the high polarity of the AO, against surface friction. However, the poleward motion in the upper troposphere acts to decrease the mean zonal flow through Coriolis force. Therefore, eddy forcing is needed to maintain, or amplify the AO. Ohhashi and Yamazaki (1999) applied an EOF analysis to the 3-dimensional wave activity flux for 500 hPa seasonal mean fields over the region from the North Atlantic to East Asia, to investigate the Eurasian pattern and found the first mode is very similar to the AO. The mechanism whereby this mode is dominant in the atmosphere, is investigated from the wave-zonal flow interaction. It is suggested that planetary-scale, stationary wavenumber three plays an important role in the dominace of the mode.

In this study, we perform the same analysis as TW98 to simulated data by an AGCM with climatological SSTs, to confirm the AO is an internal mode. The mechanism that makes the AO dominant in the atmosphere, is examined by using the transformed Eulerian-mean equation.

2. Model, experiment and analysis techniques

2.1 Model

The model used in this study is version 5.4 of the CCSR/NIES (Center for Climate System Research/National Institute for Environmental Studies) AGCM. The resolution of the model is 21 wavenumbers in horizontal, with triangular truncation and 24 levels in vertical (T21L24). The top level of the model is located at 1 hPa. The standard physics are included in the model. For the details of the model, see Numaguti *et al.* (1997).

2.2 Experiment

Two runs were made in this study. One is a standard seasonal run, with specified climatological sea surface temperatures (SSTs). The model was integrated for 20 years, starting from the motionless isothermal state. Discarding the first year, the remaining 19-year integration was used for analysis. The other integration is a perpetual February run, in which the sun and the SSTs are fixed to the values of February 15. February was chosen because the AO is most prominent in mid- and late winter (TW99a). The integration was made for 10 years, starting from the motionless isothermal state. The data for the last 9 years (3240 days) was used for analysis.

2.3 Analysis techniques

As an analysis technique, we use EOF analysis as TW98 did. The analysis domain is poleward of 20°N. In the EOF analysis, the gridded data are weighted by the square-root of the cosine of latitude to take into account the areal difference, and the eigen values and eigen vectors are calculated from a covariant matrix.

TW98 applied the EOF for SLP fields first, and then obtained the AO index as the normalized expansion coefficient. Then, regression coefficients for geopotential height fields at 500 and 50 hPa on the AO index were calculated. Kodera *et al.* (1996) applied the EOF for the geopotential height field at 50 hPa, and then regression analysis was made to 500 hPa height field, and the sea surface temperature. At the beginning we also followed TW98's method for comparison, but a combined EOF, which combines geopotential fields at 50, 500 and 1000 hPa into one field, and treats these levels equally, is used in the latter part of this paper. In the calculation of combined EOF for geopotential height fields, the data are weighted by the square-root of the density at each level to ensure that anomalies at different levels, have equal weights from the viewpoint of kinetic energy.

3. Simulated annular mode

3.1 Seasonal run

The same analysis is performed as in TW98 for the seasonal run. The leading EOF of the wintertime (November–April) monthly mean SLP (Z1000 hPa) anomaly field over the domain poleward of 20°N is shown in Fig. 1c. The simulated pattern of the leading mode, is very similar to the observed one. This mode accounts for 42 % of the variance, and the percentage is twice as large as the

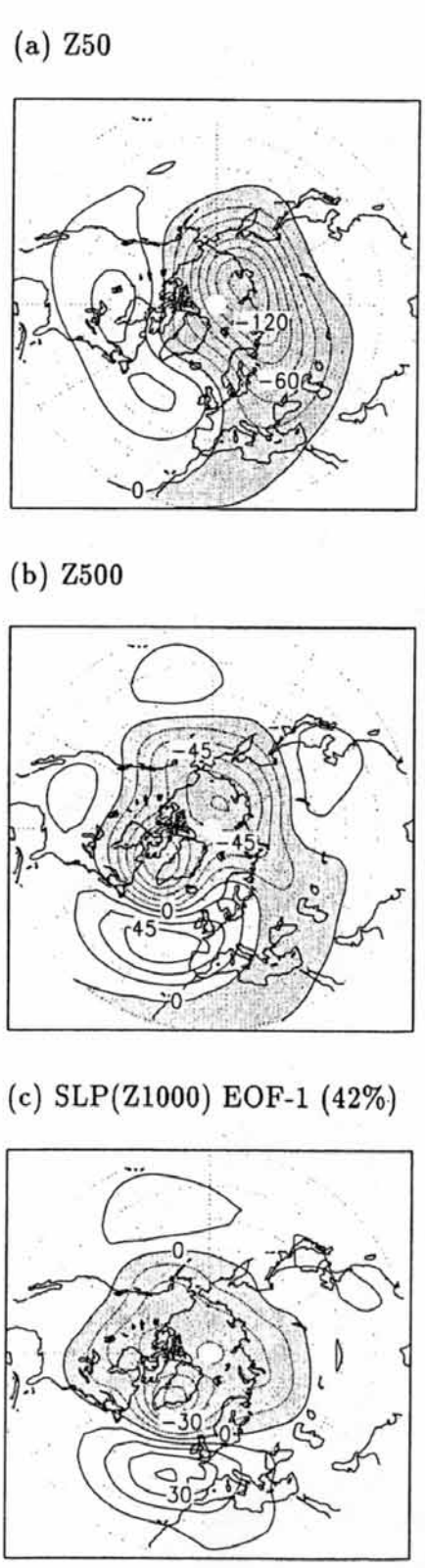

Fig. 1. The leading EOF of the wintertime (November–April) monthly-mean sea level pressure (SLP) fields simulated by the seasonal run (c). The SLP is converted to geopotential height at 1000 hPa. Regression maps for geopotential height at 50 hPa (a) and 500 hPa (b) based upon the leading EOF of SLP. Contour intervals for (a), (b) and (c) are 20 m, 15 m and 10 m, respectively. Negative values are shaded.

observed one (TW98). It is confirmed that this annular mode is an internal mode of the atmosphere. Without interannual variability of SST, the variability of the ENSO-related mode is reduced. This seems to account for the high percentage in the simulation. The regression maps for geopotential height at 50 hPa and 500 hPa are shown in Fig. 1a and 1b. These maps are similar to the observed ones, though the 50 hPa map is somewhat skewed. The simulated magnitude of this mode is also similar to the observed one, which implies that boundary forcings such as SST do not play important roles for the dominace of this mode.

The combined EOF analysis for geopotential heights at 1000 hPa, 500 hPa and 50 hPa is performed (Figures not shown). The leading combined EOF mode accounts for 32 % of the total variance and is well separated from the other eigenvalues. The second mode is a PNA-like pattern, and accounts for 12 % of the total variance. The spatial pattern of the leading mode is virtually identical to Fig. 1. Therefore, the combined EOF is used afterwards in this study. The AO index is defined in this study based upon the normalized expansion coefficient of the first combined EOF mode.

Figure 2 shows the regression map for the mean zonal wind based on the AO index, together with the first EOF of the mean zonal wind fields. This leading EOF of the mean zonal wind accounts for 46 % of the total variance. Both figures are quite similar to each other, and they are also similar to the observed one (TW99a). The AO is closely related to the seesaw-like variation of the polar vortex. Its node is located at about 40°N in the simulation. Closer inspection of Fig. 2 reveals that the zonal-mean zonal wind anomalies of the polar vortex in the model, is smaller than the observation in the stratosphere. In the model, the anomaly decreases with height above 100 hPa, while that in the observation keeps increasing (*i.e.*, TW99a). The pattern at 50 hPa in the model (Fig. 1a) is also skewed compared with observation. These facts suggest that the coupling of the stratosphere and troposphere is weak in the model.

3.2 Perpetual February run

The perpetual February run, in which the sun and the SSTs are fixed to the values on February 15, is performed. The leading combined EOF mode for 31-day running mean geopotential heights is very similar in pattern and magnitude to that for the seasonal run, and the mode accounts for 24 % of the variance. In both runs, the model successfully simulates the observed annular mode without interannual varibility of boundary forcings, and without even any change of the forcing. Therefore, it is confirmed that the AO is an atmospheric internal mode.

Even for daily-mean fields, the leading combined

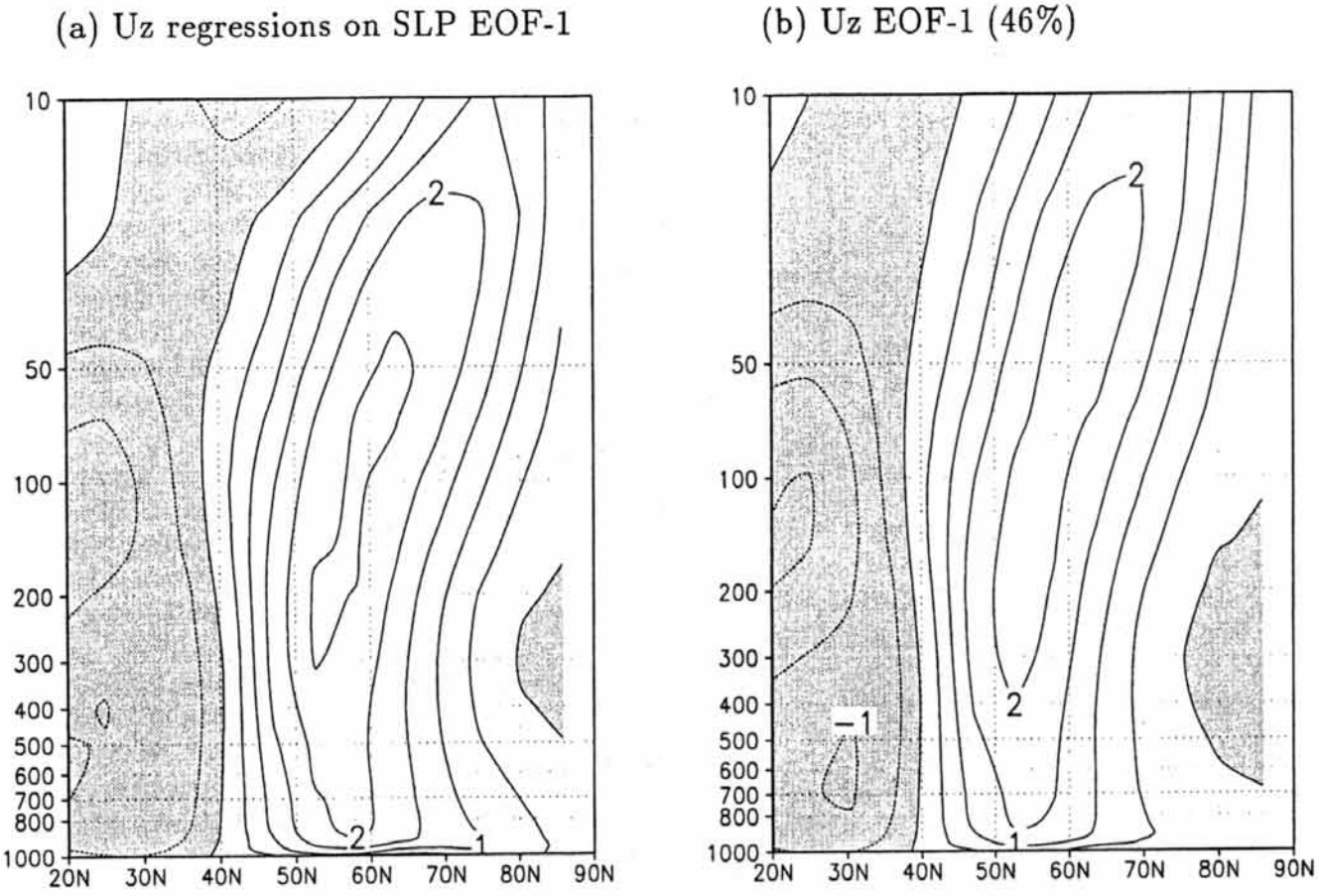

Fig. 2. (a) Regression map for zonal-mean zonal wind based upon the leading EOF of SLP (Fig. 1c) simulated by the seasonal run. (b) The leading EOF of the wintertime (November–April) monthly-mean zonal-mean zonal wind fields simulated by the seasonal run. The contour interval is 0.5 ms^{-1} and negative values are shaded.

EOF mode is similar to the observed AO (Fig. 3), though it accounts for only 12 % of the variance. The reduction of the percentage suggests that the AO becomes more dominant for longer periods, and it has persistency. Figure 4 shows the change of the lag auto-correlation coefficient of the AO index with lag. The correlation coefficient monotonically decreases with lagged day and the e-folding time is about 16 days. Time variations of the AO can be modeled as Gaussian red noise with a correlation e-folding time of about 16 days. This e-folding time is longer than that of the zonal flow vacillation in the Southern Hemisphere, which has a value of about 10 days (Hartmann and Lo, 1998). The correlation coefficient becomes negative after 37 days, and remains negative until 100 days. Although the negative values are small, they are indicative that the AO has a weak periodicity of about 4–6 months. The feature of this slow oscillation is discussed in Section 5.

4. Transition to the high/low polarity of the annular mode

To examine what causes the transition to the high/low polarity of the AO index, we make composites of the transient states, from the 3120-day perpetual February simulation. The case for the transition to the high polarity, is defined when the AO index is increasing for at least 5 consecutive days, and going beyond one standard deviation. There are 28 cases and 247 days for the transition to the high index polarity (hereafter denoted as High(↗). The transition to the low index polarity (Low(↘)) is similarly defined. There are 32 cases and 279 days for Low(↘) composite. Composite maps of 500 hPa geopotential height fields for High(↗) and Low(↘) are shown in Fig. 5. In the High(↗) case, the 500 hPa map shows a wavenumber three structure with three troughs over northern Canada, Europe and the Sea of Okhotsk. The axes of troughs over Europe and the Sea of Okhotsk seem to tilt southwestward, suggesting a poleward westerly momentum transport. In the Low(↘) case, strong ridges are evident over souhern Greenland and Alaska. The polar vortex is split into two and shifted over Hudson Bay and the Sea of Okhotsk. A wavenumber two pattern is also apparent.

Composite maps for differences of zonal-mean zonal wind between the High(↗) cases and the Low(↘) cases are shown in Fig. 6a and b for four days before the AO index exceeds one and the day when it exceeds one. The north-south dipole is evident on both days. Positive anomalies in

(a) Z50

(b) Z500

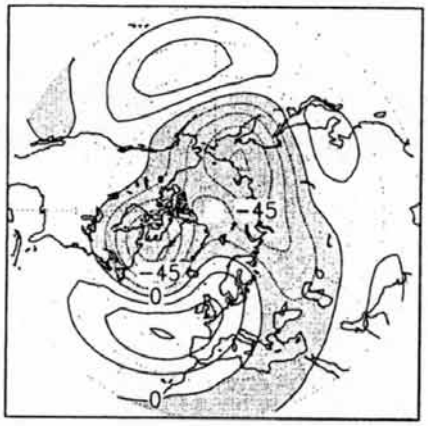

(c) Z1000

Fig. 3. The leading combined EOF of the daily-mean geopotential height fields at 50 hPa (a), 500 hPa (b) and 1000 hPa (c) simulated by the perpetual February run. Contour intervals for (a), (b) and (c) are 20 m, 15 m and 10 m, respectively. Negative values are shaded.

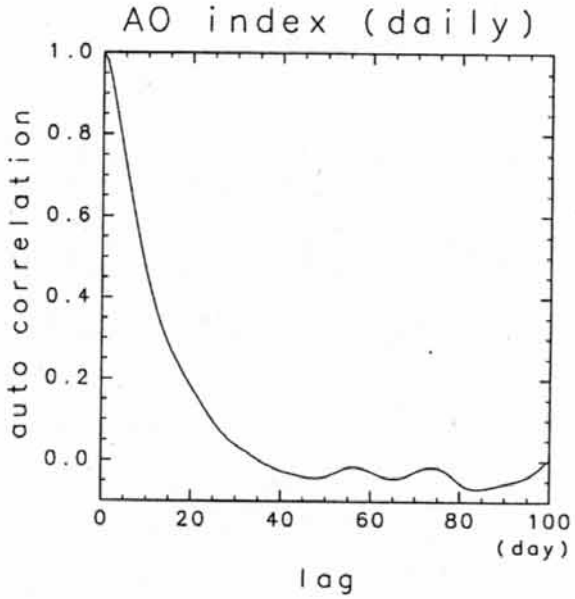

Fig. 4. Lag auto-correlation coefficient of the daily AO index simulated by the perpetual February run.

high-latitudes increase with height. The difference in wind acceleration during whole transition days (Fig. 6c), also shows the dipole pattern centered on 40°N.

The quantitative analysis is made in order to examine what enhances/weakens the polar vortex, *i.e.*, what causes the transition to the high/low polarity. To this end, we employ the transformed Euralian mean equation for the mean zonal wind. We calculated the Eliassen-Palm flux (E-P flux) and its divergence, which is the wave forcing due to eddies acting on the mean zonal flow. We also calculated the residual mean meridional velocity and the Coriolis force term including the meridional advection of mean zonal flow. The latter term also acts to change the mean zonal flow. Other terms such as vertical advection of the mean zonal flow, vertical and horizontal diffusions, and surface friction are not considered because they are small in the free atmosphere.

Figure 7a shows differences of the wave forcing and the E-P flux between High(↗) and Low(↘). This wave forcing acts to accelerate the mean zonal wind poleward of 40°N and decelerate it equatorward of 40°N in the troposphere and the lower stratosphere. On the other hand, the meridional term (Fig. 7b) acts in an opposite way in the troposphere above 700 hPa, though it acts in an somewaht similar way in the lower stratosphere. The sum of the two terms (Fig. 7c) clearly exhibits the dipole pattern of acceleration, and it accounts for the transition to the high/low polarity (see Fig. 6c for the actual acceleration of the zonal flow). Figure 7 clearly demonstrates that wave forcing due to eddies is responsible for the transition between high and low polarities and the meridional circulation tends to re-

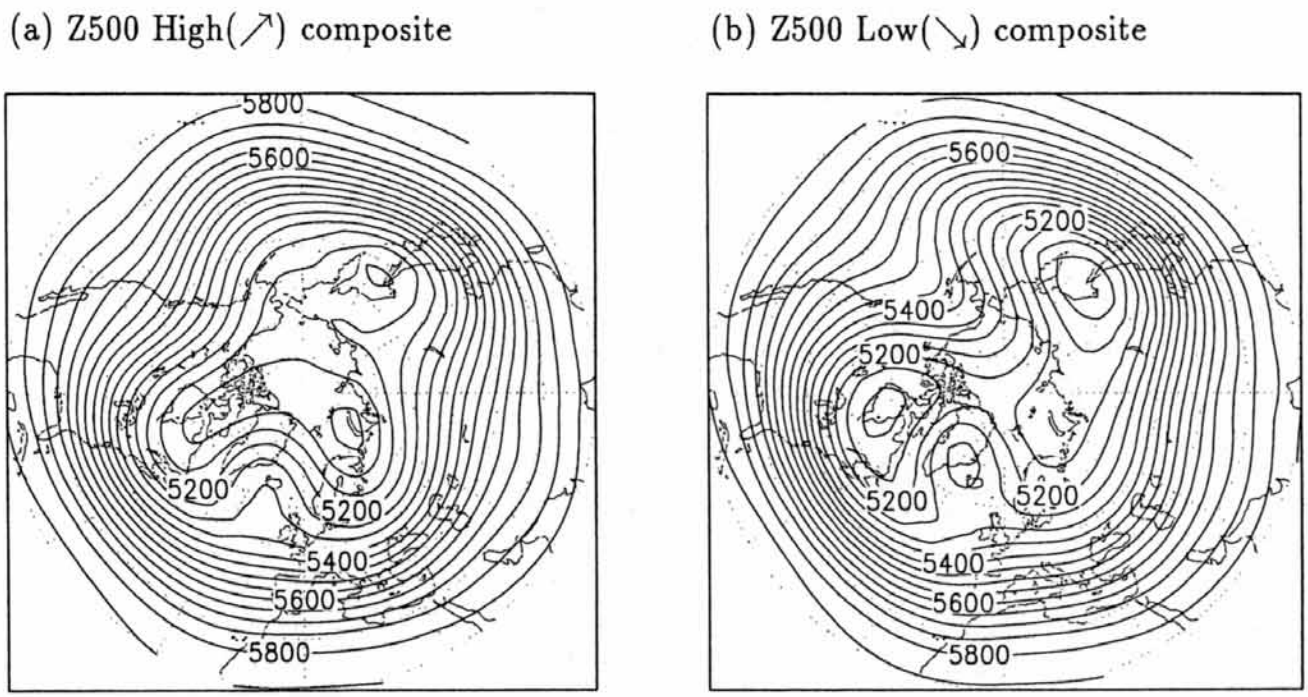

Fig. 5. Composite maps of 500 hPa geopotential height for High(↗) cases (a) and Low(↘) cases (b). The contour interval is 50 m.

store the transition. The E-P flux difference is large and equatorward in the upper troposphere.

To examine which scale of wave is responsible for the transition, the wave forcing is decomposed into zonal wave component (Fig. 8). The wavenumber one wave does not contribute to the dipole pattern of the acceleration, though the downward E-P flux anomaly is seen in the stratosphere. The synoptic-scale waves (wavenumber 4–10) do not seem to contribute either, except in the lower stratosphere between 300 hPa and 100 hPa. It acts to decelerate the mean zonal flow in low-latitudes, but it does not act to help transition in middle-latitudes. Wavenumber two and three waves contribute to the dipole pattern of the acceleration, as suggested in Fig. 5. The E-P fluxes in both waves show the equatorward propagation anomalies in the upper troposphere. Wavenumber two shows the downward anomalies in middle-latitudes. This is in the opposite direction compared with the synoptic-scale waves. When the atmosphere shifts to the high polarity state, namely, stronger polar vortex, the generation and the upward propagation of the wavenumber two wave is reduced, and the wave propagates more equatorward. The wavenumber three wave also propagates more equatorward. Anomalous equatorward E-P fluxes in middle latitudes produce the divergence of E-P flux in high latitudes, and convergence in low latitudes. The wave forcings due to these waves accelerate the mean zonal flow poleward of 40°N, and decelerate equatorward of it compared with the case for the transition to the low polarity. The generation and the upward propagation of synoptic-scale waves are enhanced, and they propagate more equatorward. From the above analysis, it is shown that the planetary-scale waves of wavenumber two and three contribute most to the dominance of the AO in the atmosphere, and synoptic-scale waves play secondary roles.

5. Summary and discussion

From the AGCM simulations, it is confirmed that the AO is an atmospheric internal mode. Even on a daily-mean basis, the AO is the leading variation mode in the atmosphere. Composite analysis based upon the perpetual February run clarified the dynamical mechanism of the transition to the high/low polarity of the AO index. Based upon the transformed Eulerian mean equation for the mean zonal wind, it is found that the wave forcing term contributes to the transition. The term of the residual meridional circulation acts to restore the transition. Among wave forcings, planetary-scale waves of wavenumber two and three are the main contributors to the transition. The synoptic-scale waves contribute partly to the low-latitude wind change.

After submission of the draft, we noticed several studies related to the AO (Baldwin and Dunkerton, 1999; Limpasuvan and Hartmann, 1999a, 1999b, personal communication; Kuroda and Kodera, 1999; Kodera and Kuroda, 1999, personal communication; Shindel *et al.*, 1999). Here, discussions on these studies are made.

Limpasuvan and Hartmann (1999a, hereafter refered as LH99a) analyzed a 100-year climatological run, *i.e.*, a seasonal run in our word, from the R30L14 version of the Geophysical Fluid Dynamics Laboratory (GFDL) GCM. The model was able

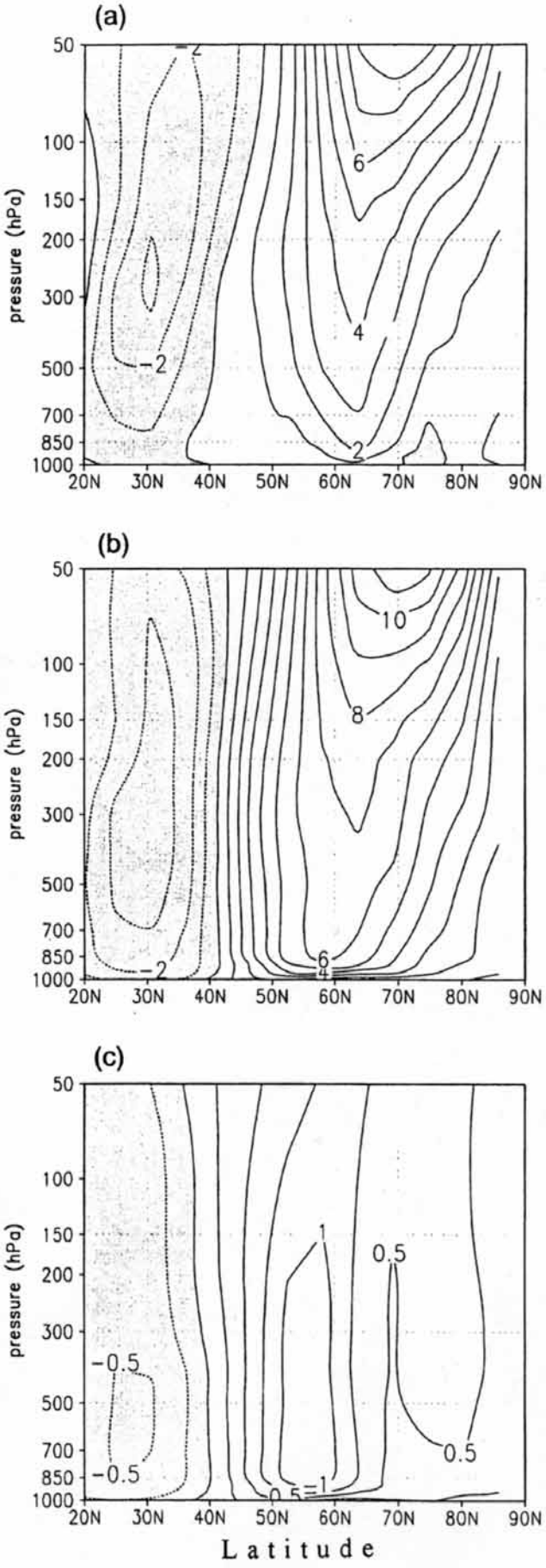

Fig. 6. Differences in zonal-mean zonal wind between the High(↗) cases and the Low(↘) cases. (a) On 4 days before the AO index exceeds one standard deviation. (b) On the day when the AO index exceeds one standard deviation. (c) Differences in zonal-mean zonal wind change. Contour intervals in (a) and (b) are 1 ms^{-1} and that in (c) is 0.25 $ms^{-1}day^{-1}$. In all panels, negative values are shaded.

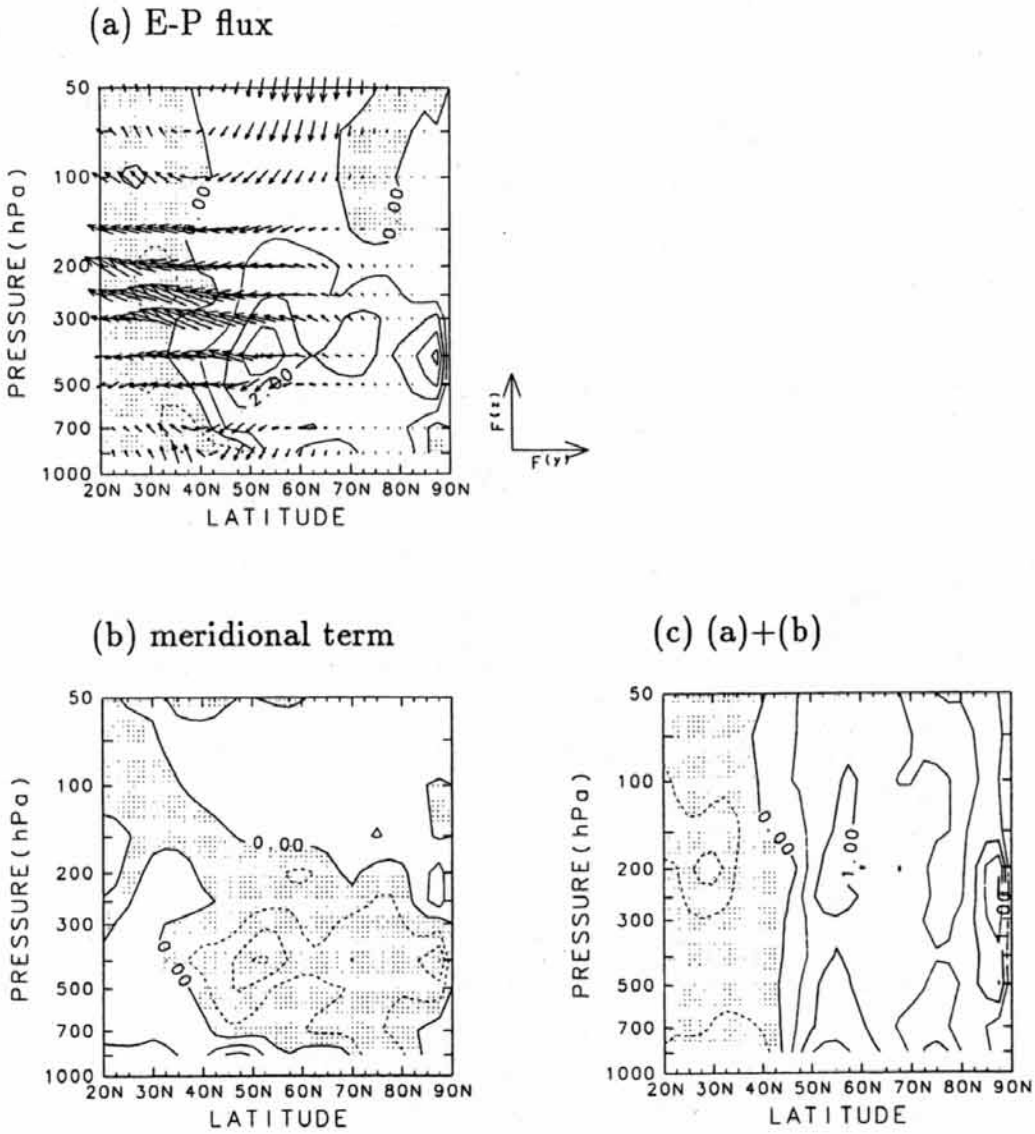

Fig. 7. Differences in E-P flux vectors and wave forcings between the High(↗) cases and the Low(↘) cases. The scale for vectors is shown at right bottom of the panel and it correponds to 1×10^{16} kg ms^{-1} in meridional component, and 2.5×10^{13} kg ms^{-1} in vertical component. Contours denote wave forcing. The contour interval is 1 ms^{-1}day^{-1} (b) Differences in the meridional term between High(↗) cases and Low(↘) case. The contour interval is 1 ms^{-1}day^{-1} (c) The sum of (a) and (b). The contour interval is 0.5 ms^{-1}day^{-1} In all panels, negative values are shaded.

to simulate the month-to-month variation of the annular modes in both hemispheres, and the role of eddies was analyzed. Both transient and stationary eddy momentum fluxes support the jet displacement in the northern annular mode (the AO). Limpasuvan and Hartmann (1999b, hereafter refered as LH99b) analyzed the above simulation and compared with the observation in detail. In our study, the distinction between transient and stationary waves was not made, because we analyzed transition periods. Waves in our study include both transient, and stationary waves. On the other hand, LH99a and LH99b did not decompose to zonal wavenumber components. We think LH99a, b and our study are complementary.

Baldwin and Dunkerton (1999, hereafter refered as BD99) analyzed the osberved data and show that AO anomalies typically appear first in the stratosphere and propagate downward into the troposphere during the cold half of a year. Kuroda and Kodera (1999, hereafter refered as KuK99) studied the slowly propagating stratosphere-troposphere coupled mode in the northern hemisphere winter based on the observation. They showed zonal-mean, zonal wind anomalies propagate poleward and downward in the stratosphere. When the anomalies reach the high-latitude region, the anomalies quickly propagate into the troposhere, and form the AO pattern. Both BD99 and KuK99 show that one or one and half cycle of the oscillation is observed during the cold half of a year when planetary waves can propagate into the stratosphere. The period of oscillation is 4–6 months. Our perpetual February simulation, suggests the existence of this slowly propagating mode as in Fig. 4. However, the slow propagating mode does not appear consistently. The

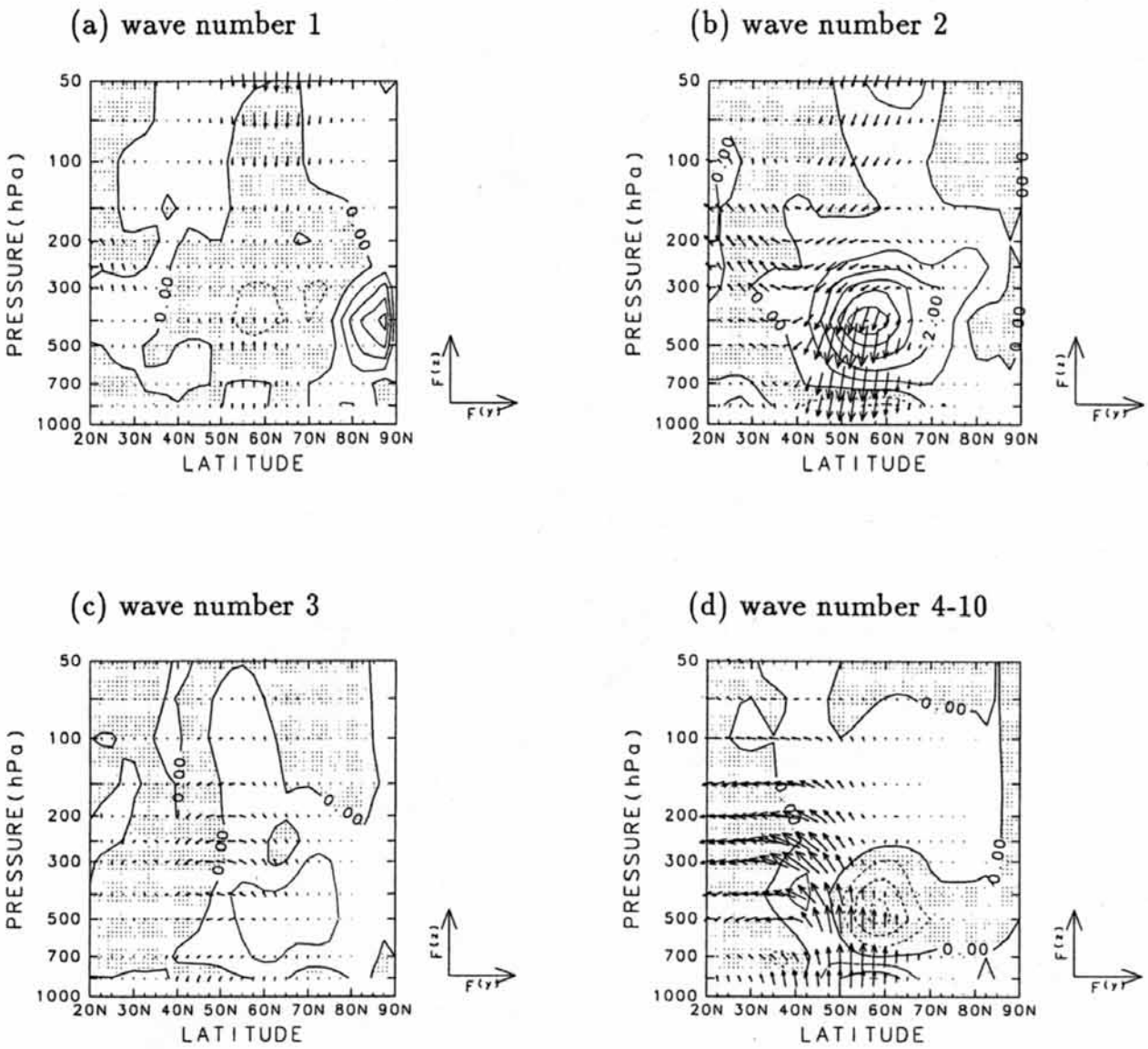

Fig. 8. As in Fig. 7a, except for each zonal wavenumber component. (a) Wavenumber 1. (b) Wavenumber 2. (c) Wavenumber 3. (d) Wavenumbers 4–10.

mode can be seen in the first, and last 1000-day periods, but it is not clearly seen in the middle 1000-day period. Figure 9 shows the 31-day running mean zonal-mean zonal wind anomaly, for the last 1000 days of the simulation. At 30 hPa (Fig. 9a) the anomaly first appears in the subtropics, and slowly propagates poleward. Once the anomaly reaches the high-latitude region, the magnitude of the anomaly becomes large. The poleward propagation becomes fast, and the anomaly propagates downward into the troposphere (Fig. 9b). The model can simulate the slow propagating AO-related mode analyzed by BD99 and KuK99 for observed data. LH99b showed the time series of the AO amplitude is equivalent to red noise, both in the model and observed data and did not detect the slow oscillation. Their analysis is based on all season data, and the top of the model is placed at 10 hPa. This means the stratosphere is not well represented in their model. The slow oscillation appears only when the stratosphere is coupled with the troposphere through planetary waves. This probably explains the lack of slow oscillating signal in LH99b.

Kodera and Kuroda (1999, personal communication, hereafter refered as KoK99) studied the slowly propagating stratosphere-troposphere coupling mode by a mechanistic model similar to Holton and Mass (1976). Their model includes two meridional Fourie components. Latitudinal variation in the gradient of the Coriolis parameter, to allow the propagation of planetary waves in meridional direction as well as in vertical direction. The lower boundary was set at the surface, and hence the troposphere is also included. The interaction between the planetary wave and zonal-mean flow produced a slow oscillation in the winter stratosphere. Zonal-wind anomalies formed in the subtropics of the stratopause propagate downward into the polar region of the troposphere. KuK99 and KoK99 pointed out an important role of wavenum-

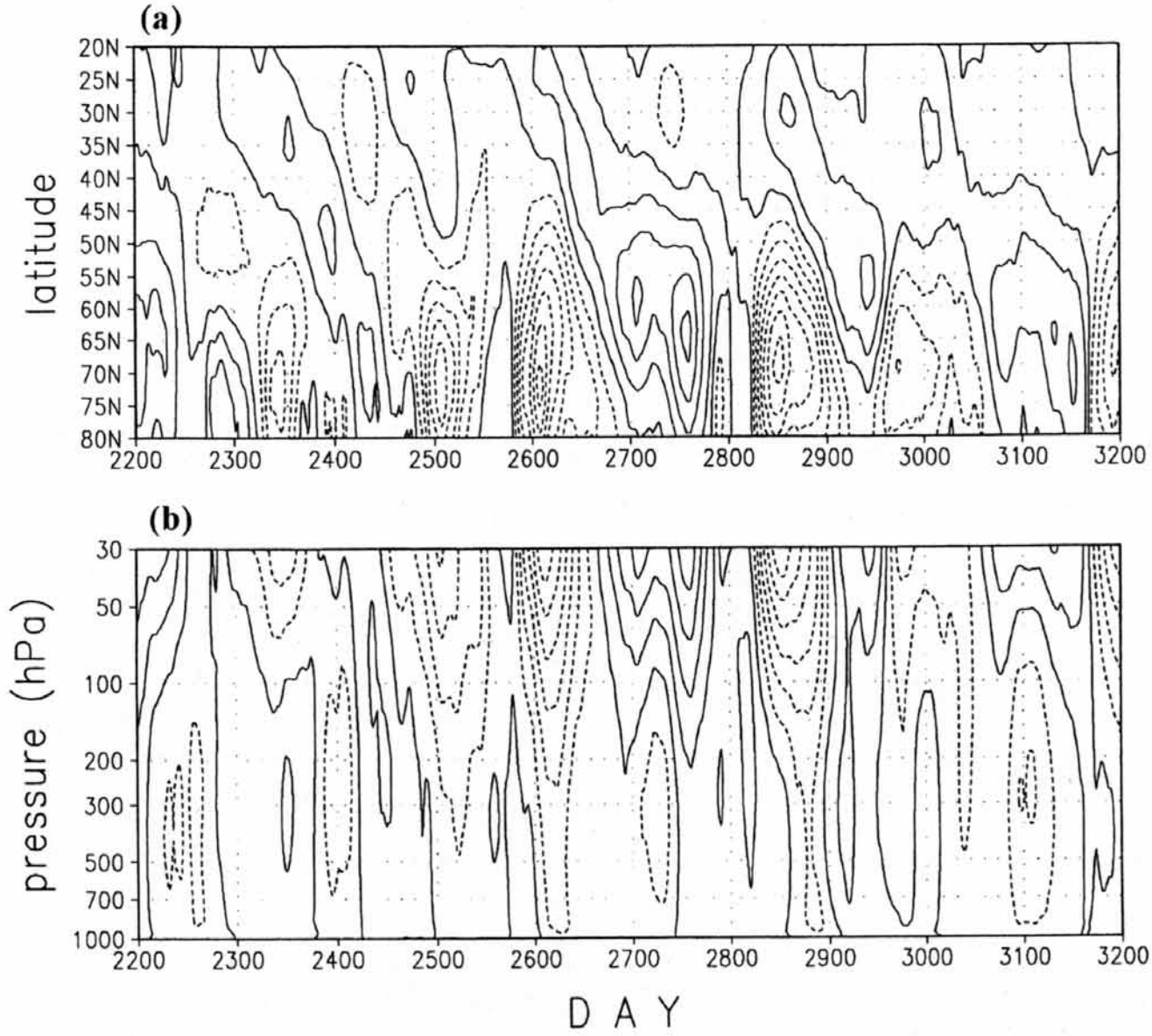

Fig. 9. (a) Time-latitude plot of zonal-mean zonal wind anomaly at 30 hPa for the last 1000 days in the perpetual February run. (b) Time-height plot of the same variable at 50–70°N. Values are low-pass filtered by a 31-day running mean. Contour interval in (a) is 4 ms^{-1} and that in (b) is 3 ms^{-1}. Negative values are shaded.

ber one, though our analysis showed wavenumver two and three waves are important for transition to high/low polarity of the AO. The top of the present model is located at 1 hPa, which might be too low to properly simulate the vertical propagation of wavenumber one wave. The other possibility is that the wavenumber one wave works efficiently in other phase of the slowly propagating mode, and wavenumber two and three waves works for the phase transition of the AO, mainly in the troposphere for shorter time-scales. Further studies are needed to clarify this point.

In the present study, we concentrated on short time-scale variation of the AO. The observed AO index after 1970s, shows a significant decadal variability and an increasing trend (TW98, Thompson and Wallace, 1999b, Koide and Kodera, 1999, Xie *et al.*, 1999). Because the dominance of the AO is caused by wave-mean flow interaction, any factors which change the zonal mean fields, or wave fields, can shift the atmospheric circulation to either the high polarity, or low polarity. Since the AO is a deep structure from the surface to the lower stratosphere, a change in the stratopheric condition might cause the change in the preferable polarity of the AO (Kodera and Yamazaki, 1994). Shindel *et al.* (1999) analyzed the global warming experiments, and showed the increasing greenhouse gase forcing is associated with the increasing trend of the AO, only when the stratosphere is included in the model. Further studies are needed to clarify what causes the increasing trend, and the decadal variation.

Acknowledgments

We express sincere thanks to Drs. Shang-Ping Xie, Hitoshi Mukougawa, Masato Shiotani, Moto Ikeda and two anonymous reviewers for their valuable comments. We express special thanks to Dr. Atusi

Numaguti for permitting us to use the CCSR/NIES AGCM. We also express our sincere thanks to Drs. Kunihiko Kodera, and Hiroshi L. Tanaka for their helpful comments and encouragements. This study is supported by the Japanese Science and Technology Agency research program on SPARC and by the Grant-in-Aid for Scientific Research of the Japanese Ministry of Education, Science, Sports and Culture. The simulation was made on HITAC M-880 at Hokkaido University and the fund from CCSR, University of Tokyo was partly used for the simulation of the model.

References

Baldwin, M.P., X. Cheng and T.J. Dunkerton, 1994: Observed correlations between winter-mean tropospheric and stratospheric circulation anomalies. *Geophys. Res. Lett.*, **21**, 1141–1144.

Baldwin, M.P. and T.J. Dunkerton, 1999: Propagation of the Arctic Oscillation from the stratosphere to the troposphere. *J. Geophys. Res.*, in press.

Hartmann, D.L. and F. Lo, 1998: Wave-driven zonal flow vacillation in the southern hemisphere. *J. Atmos. Sci.*, **55**, 1303–1315.

Holton, J.R. and C. Mass, 1976: Stratospheric vacillation cycles. *J. Atmos. Sci.*, **33**, 2218–2225.

Hurrel, J.W., 1995: Decadal trends in the North Atlantic Oscillation: Regional temperature and precipitation, *Science*, **269**, 676–679.

Kitoh, A., H. Koide, K. Kodera, S. Yukimoto and A. Noda, 1996: Interannual variability in the stratospheric-tropospheric circulation in a coupled ocean-atmosphere GCM. *Geophys. Res. Lett.*, **23**, 543–546.

Kodera, K. and K. Yamazaki, 1994: A possible influence of recent polar stratospheric coolings on the troposphere in the northern hemisphere winter. *Geopys. Res. Lett.*, **21**, 809–812.

Kodera, K., M. Chiba, H. Koide, A. Kitoh and Y. Nikaidou, 1996: Interannual variability of winter stratosphere and troposphere in the northern hemisphere. *J. Meteor. Soc. Japan*, **74**, 365–382

Koide, H. and K. Kodera, 1999: A SVD analysis between the winter NH 500-hPa height and surface temperature fields. *J. Meteor. Soc. Japan*, **77**, 47–61.

Kuroda, Y. and K. Kodera, 1999: Role of planetary waves in the stratosphere-troposphere coupled variability in the northern hemisphere winter. *Geophys. Res. Lett.*, **26**, 2375–2378.

Limpasuvan, V. and D.L. Hartmann, 1999a: Eddies and the annular modes of climate variability. *Geophys. Res. Lett.*, **26**, 3133–3136.

Numaguti, A., M. Takahashi, T. Nakajima and A. Sumi, 1997: Description of CCSR/NIES atmospheric circulation model. *CGER's Supercomputer Monograph Report, Center for Global Environmental Research, National Institute for Environmental Studies*, **No. 3**, 1–48.

Ohhashi, Y. and K. Yamazaki, 1999: Variability of the Eurasian pattern and its interpretation by wave activity flux. *J. Metero. Soc. Japan*, **77**, 495–511.

Perlwitz, J. and H.-F. Graf, 1995: The statistical connection between tropospheric and stratopsheric circulation of the Northern Hemisphere in winter. *J. Climate*, **8**, 2281–2295.

Shindel, D.T., R.L. Miller, G.V. Schmidt and L. Pandolfo, 1999: Simulation of recent northern winter climate trends by greenhouse gas forcing. *Nature*, **399**, 452–455.

Thompson, D.W. and J.M. Wallace, 1998: The Arctic Oscillation signature in the wintertime geopotential height and temperature fields. *Geophys. Res. Lett.*, **25**, 1297–1300.

Thompson, D.W. and J.M. Wallace, 1999a: Annular modes in the extratropical circulation. Part I: Month-to-month variability. *J. Climate*, in press.

Thompson, D.W. and J.M. Wallace, 1999b: Annular modes in the extratropical circulation. Part II: Trends. *J. Climate*, in press.

Xie, S.-P., H. Noguchi and S. Matsumura, 1999: A hemispheric-scale quasi-decadal oscillation and its signature in northern Japan. *J. Meteor. Soc. Japan*, **77**, 573–582.